JVI Journals.ASM.org

Single-Domain Antibody-SH3 Fusions for Efficient Neutralization of HIV-1 Nef Functions

Jérôme Bouchet,[a,b] Cécile Hérate,[a,b] Carolin A. Guenzel,[a,b] Christel Vérollet,[c,d] Annika Järviluoma,[e] Julie Mazzolini,[a,b] Salomeh Rafie,[a,b] Patrick Chames,[f] Daniel Baty,[f] Kalle Saksela,[e] Florence Niedergang,[a,b] Isabelle Maridonneau-Parini,[c,d] and Serge Benichou[a,b]

Institut Cochin, CNRS (UMR8104), Université Paris Descartes, Paris, France[a]; INSERM U1016, Paris, France[b]; Institut de Pharmacologie et de Biologie Structurale, CNRS (UMR5089), Toulouse, France[c]; Université Paul Sabatier, Institut de Pharmacologie et de Biologie Structurale, Université de Toulouse, Toulouse, France[d]; Department of Virology, Haartman Institute, Helsinki University Central Hospital, University of Helsinki and HUSLAB, Helsinki, Finland[e]; and INSERM U624, Marseille, France[f]

HIV-1 Nef is essential for AIDS pathogenesis, but this viral protein is not targeted by antiviral strategies. The functions of Nef are largely related to perturbations of intracellular trafficking and signaling pathways through leucine-based and polyproline motifs that are required for interactions with clathrin-associated adaptor protein complexes and SH3 domain-containing proteins, such as the phagocyte-specific kinase Hck. We previously described a single-domain antibody (sdAb) targeting Nef and inhibiting many, but not all, of its biological activities. We now report a further development of this anti-Nef strategy through the demonstration of the remarkable inhibitory activity of artificial Nef ligands, called Neffins, comprised of the anti-Nef sdAb fused to modified SH3 domains. The Neffins inhibited all key activities of Nef, including Nef-mediated CD4 and major histocompatibility complex class I (MHC-I) cell surface downregulation and enhancement of virus infectivity. When expressed in T lymphocytes, Neffins specifically inhibited the Nef-induced mislocalization of the Lck kinase, which contributes to the alteration of the formation of the immunological synapse. In macrophages, Neffins inhibited the Nef-induced formation of multinucleated giant cells and podosome rosettes, and it counteracted the inhibitory activity of Nef on phagocytosis. Since we show here that these effects of Nef on macrophage and T cell functions were both dependent on the leucine-based and polyproline motifs, we confirmed that Neffins disrupted interactions of Nef with both AP complexes and Hck. These results demonstrate that it is possible to inhibit all functions of Nef, both in T lymphocytes and macrophages, with a single ligand that represents an efficient tool to develop new antiviral strategies targeting Nef.

The Nef protein of HIV-1 promotes virus replication and is essential for the pathogenesis of AIDS. This essential role of Nef results from its ability to disrupt certain intracellular trafficking and signaling pathways in infected cells (for a review, see references 1 and 9). Nef is indeed a multifunctional protein that is able to interact with components involved in vesicular transport between membrane compartments of the endocytic pathway and in the control of intracellular signaling pathways. These interactions are related to the presence of specific motifs that are reminiscent of specific interaction motifs found in cellular proteins within the primary sequence of HIV-1 Nef. Two types of motifs of Nef have been extensively analyzed: a leucine-based motif (E/D_{160}xxxLL_{165}), found in a C-terminal flexible loop of HIV-1 Nef, and a polyproline (poly-Pro; P_{72}xxP_{75}) motif. While the leucine-based motif allows the recruitment of clathrin-associated adaptor protein (AP) complexes that participate in vesicular transport within the endocytic pathway, the polyproline motif is required for interactions with cellular proteins containing SH3 domains, such as tyrosine kinases of the Src family (for a review, see reference 22). Therefore, some functions of Nef, such as the cell surface downmodulation of certain surface receptors, including CD4, are specifically dependent of the Leu-based motif, whereas the integrity of the polyproline motif is required for some other Nef effects, such as the intracellular redistribution of the Src kinase Lck, which is observed in HIV-1-infected T cells (12). Interestingly, the Nef-mediated enhancement of HIV-1 infectivity depends on the integrity of both Leu-based and polyproline motifs (24, 35).

Nef is abundantly expressed early after virus infection and perturbs the trafficking of several transmembrane proteins through alterations of the endocytic pathway. This leads to the modulation of the cell surface expression of cellular receptors, including CD4 and major histocompatibility complex class I (MHC-I) molecules, both in CD4-positive T cells and macrophages (20, 36). While the Nef-mediated modulation of CD4 requires the C-terminal AP-binding Leu-based motif, MHC-I downmodulation is determined by distinct motifs located in the N-terminal part of Nef, an acidic cluster (E_{62}EEE$_{65}$) and the poly-Pro SH3-binding motif (P_{72}xxP_{75}), indicating that the Nef-mediated cell surface downregulation of either CD4 or MHC-I is related to different mechanisms (reviewed in reference 22).

In addition to T cells, macrophages represent important targets of HIV-1 during the initial steps of infection, and they contribute to the establishment of viral reservoirs even in patients under highly active antiretroviral therapy (reviewed in reference 10). Infected macrophages also participate in the propagation of virus in nonlymphoid tissues, such as lungs or brain. Furthermore, we have recently shown that Nef expression during HIV-1 infection disturbs specialized functions of macrophages: (i) Nef induces the fusion of infected macrophages, leading to the formation of multinucleated giant cells through the activation of the Hck tyrosine kinase (40), and (ii) Nef also inhibits phagocytosis through the

Received 16 September 2011 **Accepted** 3 February 2012
Published ahead of print 15 February 2012
Address correspondence to Serge Benichou, serge.benichou@inserm.fr.
C. H., C.A.G., and C. V. contributed equally to this article.

doi:10.1128/JVI.06329-11

alteration of the polarized exocytosis of recycling endosomes regulated by AP-1 (28).

Specifically expressed in phagocytes, the Nef-targeted Hck kinase is present in macrophages in two isoforms: p59Hck is found at the plasma membrane and induces the formation of F-actin-rich protrusions, whereas p61Hck is localized at the membrane of lysosomes, where it can induce the formation of podosome rosettes (6, 11). Nef is able to activate both Hck isoforms, leading to the formation of actin-rich protrusions and podosome rosettes (43). By activating p61Hck, Nef also triggers the fusion of individual infected macrophages, leading to the formation of giant multinucleated cells that could contribute to the establishment of latent virus reservoirs in some tissues (40). In addition, we recently showed that Nef expression in HIV-1-infected macrophages also resulted in a significant diminution of their phagocytosis ability (28). This defect of phagocytosis did not involve the downregulation of phagocytosis-involved receptors, but we observed a decrease of AP-1-positive endosome recruitment at the phagocyte cup (28).

While it is well established that Nef is essential for AIDS pathogenesis, it is not currently targeted by antiviral therapeutic strategies. The first Nef inhibitor described in the literature was based on the inhibition of the Nef interaction with an optimized derivative of the SH3 domain of Hck (16). More recently, small Nef-interacting proteins composed of a Nef-targeted SH3 domain, fused to a sequence motif of the CD4 cytoplasmic tail and combined with a prenylation signal for membrane association, also have been developed (4). SH3 domains are conserved structures composed of five β leaflets that are organized in two superposed surfaces and linked with unstructured loops (18, 27). The first loop, called the RT loop, is critical for recognition by HIV-1 Nef (23). To characterize Nef inhibitors, we previously generated an SH3 domain library in which the RT loop was replaced by a random hexapeptide (RRT, for random RT loop), and we isolated RRT-SH3 peptides that bound Nef with high affinity (dissociation constant $[K_d] = 7$ nM) (4, 15, 16).

We have recently described a single-domain antibody (sdAb) that binds Nef with high affinity ($K_d = 2$ nM) and inhibits most of the functions of Nef in CD4-positive T lymphocytes (3). This antibody fragment, called sdAb19, is able to counteract the Nef-mediated endocytosis of CD4 from the cell surface, and it also inhibits the positive effect of Nef on viral replication and infectivity (21). Finally, sdAb19 is also active *in vivo* by rescuing Nef-mediated thymic $CD4^+$ T-cell maturation defects and peripheral $CD4^+$ T-cell activation in a CD4c/HIV-1^{Nef} transgenic mouse model (13). However, sdAb19 does not inhibit the Nef-mediated downregulation of MHC-I molecules (3), probably because it is not able to target the Nef residues involved in this function.

Here, we aimed to further improve the inhibitory activity of sdAb19 by expression as fusions with RRT-SH3 peptides (RRT loop) that were previously selected for binding to Nef with high affinity (16). Two chimeric constructs, called Neffins, have been generated, and they were able to potently inhibit all of the functions of Nef that we tested, including the cell surface downregulation of MHC-I. When expressed in T cells, Neffins specifically inhibited the Nef-mediated mislocalization of the Lck kinase that is involved in the Nef-induced impairment of the organization and function of the immunological synapse. In macrophages, Neffins inhibited the Nef-induced formation of multinucleated cells and rescued the inhibitory activity of Nef on phagocytosis through the disruption of interactions of Nef with both AP complexes and Hck.

MATERIALS AND METHODS

Plasmids. Plasmids encoding wild-type or mutated Nef-hemagglutinin (Nef-HA) and Nef-green fluorescent protein (Nef-GFP), as well as a plasmid for the expression in bacteria of Nef fused to glutathione *S*-transferase (GST), have been described previously (20, 24). Plasmids for the expression of sdAb19 (pET-sdAb19) in bacteria and in mammalian (pCDNA3.1-sdAb19) cells were also described already (2). Plasmids for the expression of Neffin B6 and Neffin C1 in mammalian cells were constructed by transferring an RRT-SH3 (B6 or C1) DNA fragment, amplified by PCR using specific primers, from the vector pEBB-myr-GST-RRT-SH3 (15, 16) into the NotI site of the sdAb19-pCDNA3 vector. For expression in bacteria, Neffins were amplified by PCR using specific primers and then subcloned in pET15b as described previously (2).

Cell culture and transfection. 293T, HeLa, CEM, HPB-ALL, Jurkat, THP-1, and RAW264.7 cell lines were grown and transfected as previously described (2, 28, 36).

Immunofluorescence analysis. The immunofluorescence of HeLa cells was done as described previously (2), and cells were examined under an inverted Leica DMI6000 microscope equipped with a spinning disk (Yokogawa CSU-X1M1), a 63× oil immersion objective, and a cooled charge-coupled device camera (CoolSnap HQ2; Photometrics). Images were analyzed and processed with ImageJ (National Institutes of Health) and Photoshop (Adobe System Inc.). To represent the colocalization of the two proteins in white (Fig. 1B), the ImageJ colocalization plug-in was used. To quantitatively evaluate the level of the colocalization of the two proteins, we calculated the Pearson's correlation coefficient (25) with the ImageJ JACoP plug-in (2) for at least 10 independent cells.

Immunofluorescence on Jurkat T cells was determined as described previously (37). Briefly, Jurkat cells were permeabilized with 0.1% Triton X-100 and then stained with anti-Lck (MAb 3A5; Santa Cruz Biotech) and anti-c-Myc (71D10; Cell Signaling Technology) primary antibodies, followed by CY3- and Alexa 647-labeled secondary antibodies, respectively. Cells were examined under a confocal Zeiss LSM700 microscope using a 63× objective. To quantify Lck mislocalization, 3 independent experiments were carried out and 50 cells of each condition were counted. Results are expressed as the percentage of transfected cells with Lck relocated in an intracellular compartment compared to total counted transfected cells.

Immunostaining in RAW264.7 cells was done as previously described (40), and fluorescent cells were visualized using a Leica DM-RB fluorescence microscope. For the analysis of cell fusion, cells were examined 48 h after transfection in areas with similar cell density. All cells were counted, and the cell fusion index was calculated with the following formula: total number of nuclei in macrophage giant cells (cells with ≥2 nuclei) divided by the total number of nuclei times 100. For each condition, at least 200 cells were counted (40). For the analysis of podosome rosette formation, slides were coated with vitronectin (Sigma), and 100 U/ml recombinant mouse gamma interferon (IFN-γ) (Peprotech) was added 8 h after transfection as described previously (40). Cells were then examined 16 h later. Statistically differences were determined using the Student's *t* test, and differences were considered significant for $P < 0.01$ (**) or $P < 0.001$ (***).

Phagocytosis assay. The phagocytosis of red blood cells (RBCs) or zymosan was performed on transfected RAW264.7 macrophages as described previously (28). To quantify phagocytosis, the number of internalized particles (RBCs or zymosan) was counted at 60 min in 50 cells randomly chosen on the coverslips, and the phagocytic index (i.e., the mean number of phagocytosed particles per cell) was calculated. The index obtained for transfected cells was divided by the index obtained for control cells (negative cells of the same coverslip) and expressed as a percentage of control cells. We also counted the number of initial cell-associated particles (at 3 min) and calculated the association index (mean

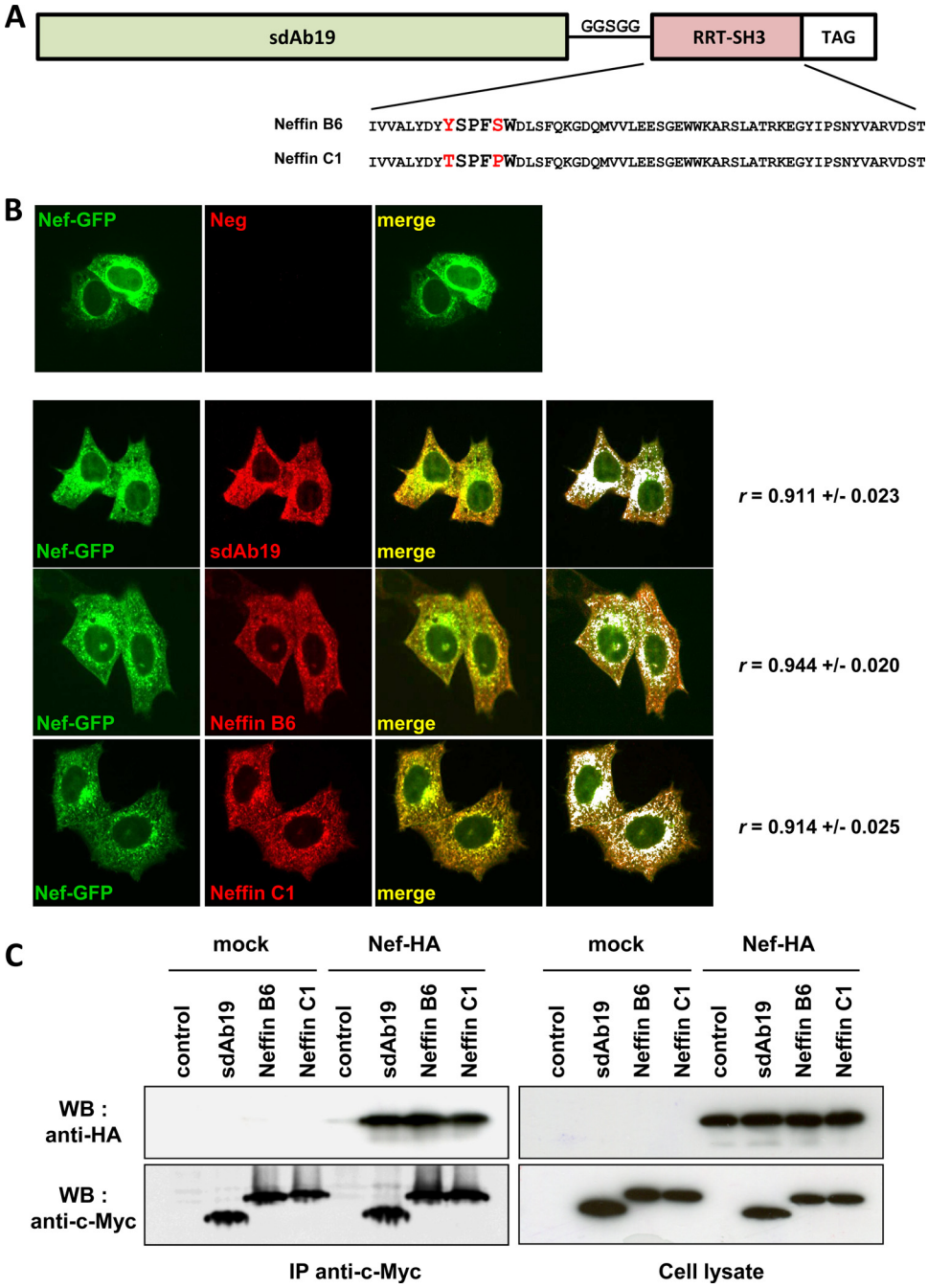

FIG 1 Association of sdAb19 and Neffins with Nef. (A) Schematic representation of Neffins resulting from the fusion of sdAb19 to RRT-SH3 B6 or C1 domain (highlighted) using a flexible GGSGG loop. TAG, c-Myc-epitope tag. (B) Intracellular distribution of Nef-GFP and sdAb19, Neffin B6, or C1. HeLa cells were transfected with the plasmid for the expression of the c-Myc-tagged sdAb19 or Neffins in combination with the plasmid for the expression of Nef-GFP. SdAb19 and Neffins were detected by indirect immunofluorescence with anti-c-Myc. The colocalization of Nef-GFP with sdAb19 and Neffins B6 and C1 is shown in white (right panels), and the Pearson's coefficient (*r*) for the evaluation of the level of colocalization is indicated on the right. (C) Coimmunoprecipitation of Nef-HA with sdAb19 or Neffins. 293T cells were transfected with the plasmid for the expression of the c-Myc-tagged sdAb19 or Neffins in combination with the plasmid for the expression of either Nef-HA or HA (mock). Control corresponds to cells that did not express sdAb19 or Neffins. Cell lysates (right images) were submitted to immunoprecipitation with anti-c-Myc (left images). Immunoprecipitates were analyzed by Western blotting (WB) using anti-c-Myc (bottom) or anti-HA (top). IP, immunoprecipitation.

number of associated particles per cell), and we expressed it as a percentage of control cells (i.e., negative cells of the same coverslip).

Viral production and infectivity assay. Single-round HIV-1 carrying the GFP gene virus particles was produced in 293T cells as described previously (21). The infectivity of HIV-1 HXBc2 and vesicular stomatitis virus G envelope glycoprotein (VSV-G)-pseudotyped viruses was analyzed on HPB-ALL T cells as described previously (21).

Immunoprecipitation and immunoblot analysis. Immunoprecipitations were carried out on lysates of transfected 293T cells as described previously (2, 21) using anti-c-Myc (clone 9E10; Roche) anti-

bodies. Immunoprecipitated proteins then were analyzed by Western blotting with anti-c-Myc and anti-HA (sc-8334; Santa Cruz) as described previously (2, 21).

Nef-induced CD4 and MHC-I downregulation. Transfected HPB-ALL T cells were stained at 4°C with phycoerythrin (PE)-conjugated anti-HLA-A2 for MHC-I or PE-CY5-conjugated anti-CD4 (clone RPA-T4; BD Biosciences), and cell surface expression was measured by flow cytometry as described previously (5). Results were expressed as the percentage of the mean fluorescence intensity determined in GFP-positive cells relative to that determined in GFP-negative cells.

GST pulldown assay. GST-Nef, sdAb19, and Neffins were produced in *Escherichia coli* strain BL21 as described previously (19, 28). Briefly, 1 nmol of recombinant GST or GST-Nef was immobilized on 30 μl of glutathione-Sepharose beads (GE Healthcare) and incubated for 1 h at 4°C with 1, 3, or 9 nmol of recombinant sdAb19, Neffin B6, or Neffin C1. Beads were washed twice in PBS and then incubated with 1 mg of THP-1 cell lysate for 3 h at 4°C as described previously (28). Bound material was analyzed by Western blotting. Immunoblots against AP-1 and Hck were performed using mouse monoclonal anti-γ-adaptin (100/3; Sigma-Aldrich) and rabbit-polyclonal anti-Hck (SC-72; Santa Cruz Biotechnology), respectively.

RESULTS

Interactions between Nef and Neffins in cells. To improve the inhibitory activity of the anti-Nef sdAb19 and to expand its activity against the multiple functions of Nef, we generated two chimeric proteins in which the parental sdAb19 was fused to the N-terminal end of SH3 polypeptides previously selected for high-affinity binding to HIV-1 Nef (16). These polypeptides were derived from the macrophage-specific Hck kinase, but they carried substitutions within a hexapeptide region in the RT loop of this SH3 domain (Neffins B6 and C1) (Fig. 1A). A more complete description of the design and biochemical properties of Neffins will be described elsewhere (A. Järviluoma, T. Strandin, S. Lulf, J. Bouchet, A. R. Makela, M. Geyer, S. Benichou, and K. Saksela, unpublished data).

As described for the parental sdAb19 (2), we first examined the ability of sdAb19-SH3 Neffins to target Nef by immunofluorescence investigation in HeLa cells expressing Myc-tagged Neffins in combination with Nef-GFP (Fig. 1B). When expressed alone (data not shown), both Neffins and sdAb19 were randomly distributed between the nucleus and the cytoplasm of transfected cells. In Nef-GFP-expressing cells (Fig. 1B), Neffin B6 or Neffin C1, as well as sdAb19, was redistributed to the cytoplasm and colocalized with the dotted Nef-positive structures concentrated in the perinuclear region, corresponding to the endosomal compartments described previously (24). The calculation of the Pearson's coefficient (r) to evaluate the level of colocalization between Nef-GFP and sdAb19, Neffin B6, or Neffin C1 gave rise to high r values (0.911, 0.944, and 0.914, respectively). Interestingly, the level of colocalization with Nef-GFP was significantly higher in cells coexpressing Neffin B6 than in cells expressing Neffin C1 ($P = 0.03$) or sdAb19 ($P = 0.02$) as evaluated by the Pearson's coefficient.

To confirm that this colocalization was due to direct interactions between Nef and Neffins, coimmunoprecipitation analyses were performed on cells coexpressing c-Myc-Neffins and HA-tagged Nef (Fig. 1C). Using anti-c-Myc antibody, Nef-HA was efficiently and specifically coprecipitated with either sdAb19, Neffin B6, or Neffin C1. These results indicate that Neffins are functional in the intracellular environment and can efficiently associate with coexpressed Nef protein. Under these conditions, the additional Nef-binding interface provided by the SH3 domain did not have an obvious effect on the amount of coprecipitated Nef.

Neffins do inhibit both CD4 and MHC-I cell surface downregulation. Having established that Nef was efficiently recognized by Neffins B6 and C1, the Neffins were subjected to a thorough analysis regarding their inhibitory potential on the best-characterized functions of Nef, including the cell surface downregulation of CD4 and MHC-I. Because sdAb19 was not able to inhibit MHC-I downregulation (Fig. 2A) (2), we first investigated whether the SH3 fusion could provide the Neffins with the capacity to inhibit this Nef function. As shown in Fig. 2A, Nef-GFP efficiently downregulated MHC-I from the surface of transfected T cells, and the poly-Pro motif of Nef was required for this Nef activity, since MHC-I downregulation was abrogated when the two proline residues were mutated to alanines (NefPxxP/AxxA mutant). When cells were cotransfected with Nef-GFP and increasing amounts of Neffin B6- or C1-encoding plasmids (1:1 to 1:3 ratios), MHC-I downregulation by Nef was inhibited in a dose-dependent manner, leading to the restoration of cell surface levels of MHC-I molecules equivalently to that measured in the absence of Nef (Fig. 2A and B).

Similar studies of the Nef-induced downregulation of the cell surface expression of CD4 (Fig. 2C) or CCR5 (data not shown) showed that both Neffins B6 and C1 were able to inhibit these Nef effects in a dose-dependent manner. However, no obvious increase in their potency in blocking CD4 and CCR5 downregulation could be seen compared to that of the parental sdAb19. Where cell surface CD4 was plotted as a function of GFP fluorescence, the inhibition of the CD4 downregulation activity by sdAb19 or Neffins was efficient even at the highest level of Nef expression. Similarly, CD4 downregulation could be efficiently neutralized by sdAb19 and Neffins when the expression of the native Nef protein was driven by the HIV-1 long terminal repeat (LTR) promoter (data not shown). Finally, we checked that the inhibitory effects provoked by increasing amounts of sdAb19 or Neffin expression were not due to a decrease of Nef-GFP expression, as evidenced by Western blot analysis (data not shown).

Interestingly, Neffin B6 was able to inhibit the CD4 downregulation activity of some Nef alleles, such as Nef proteins from the NA7 or YBF30 HIV-1 strains, that were not affected by the coexpression of sdAb19 (Fig. 2D, left) (2). The MHC-I downregulation activity of these Nef proteins was also counteracted in cells coexpressing Neffin B6 (Fig. 2D, left). Taken together, these results show that Neffins are potent inhibitors of the cell surface downregulation of two major cellular targets of Nef. They also indicate that Neffins display a broader inhibitory activity than the parental sdAb19 against a very large panel of HIV-1 Nef proteins.

Neffins specifically inhibit the Nef-induced mislocalization of the Lck kinase. While it has been shown that Nef expression impairs the ability of infected T lymphocytes to form immunological synapses with antigen-presenting cells, this effect was related, at least in part, to a mislocalization of the T cell receptor (TCR)-proximal Lck kinase in endosomal compartments (34, 37). Since this mislocalization of Lck specifically depends on the poly-Pro motif of Nef (12), we investigated by immunofluorescence analysis whether Neffins were able to counteract the intracellular redistribution of Lck observed in T cells expressing Nef-GFP. As shown in Fig. 3A, Lck was mainly localized at the plasma membrane in control cells expressing GFP. In contrast, the expression of Nef-GFP resulted in a net redistribution of Lck which accumulated in an intracellular compartment (Fig. 3A), and the poly-Pro motif of

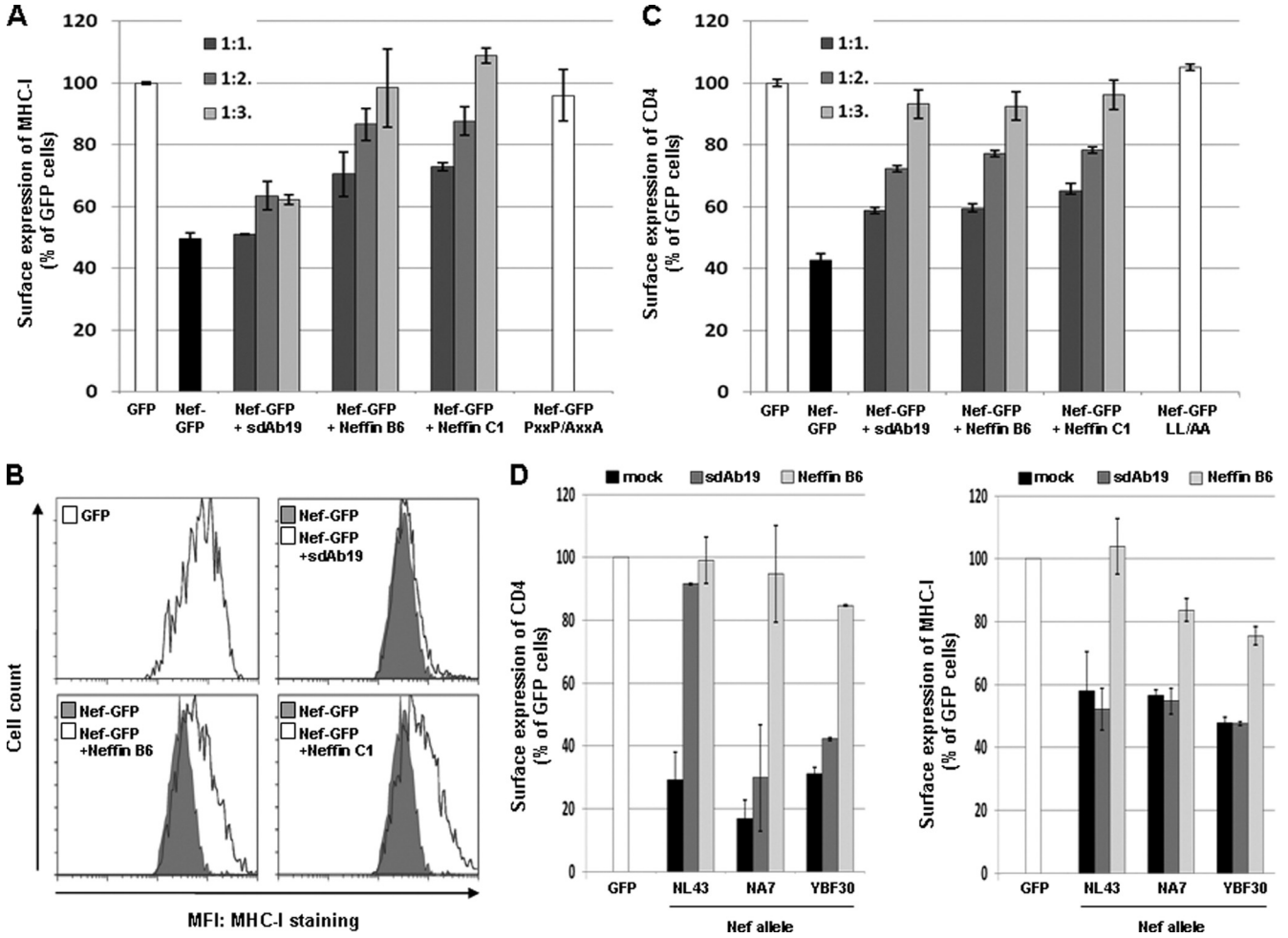

FIG 2 Neffins inhibit Nef-induced MHC-I and CD4 downregulation. (A to C) HPB-ALL T cells were transfected with plasmids for the expression of either Nef-GFP (NL43 allele) or GFP in combination with increasing amounts of the plasmid for the expression of sdAb19 or Neffins as indicated. Transfected cells were stained with PE-conjugated anti-HLA-A (A and B) or PE-conjugated anti-CD4 (C) at 4°C, and the surface expression of MHC-I or CD4 in Nef-GFP- or GFP-expressing cells was measured by flow cytometry. The PxxP/AxxA and NefLL/AA mutants were used as controls. (D) Cells were transfected (1:3) with the plasmid for the expression of sdAb19 or Neffin B6 in combination with the plasmid for the expression of the indicated Nef protein (NL43, NA7, or YB30 allele) expressed as GFP fusions. The surface expression of MHC-I (right graphs) or CD4 (left graphs) in Nef-GFP- or GFP-expressing cells then was assessed as indicated above. Results are expressed as the percentage of the mean fluorescence intensity (MFI) determined in GFP-positive cells relative to that determined in GFP-negative cells. Values are the means from at least 3 independent experiments. Error bars represent 1 standard deviation (SD) from the means.

Nef, but not the Leu-based motif, was required for this Nef activity (Fig. 3B). When cells were cotransfected with Nef-GFP and Neffin B6- or C1-encoding plasmids (1:1 ratio), the mislocalization of Lck induced by Nef was largely inhibited, leading to the restoration of plasma membrane Lck staining almost equivalently to that observed in the absence of Nef (Fig. 3A and B). In contrast, sdAb19 failed to counteract the Nef-induced mislocalization of Lck (Fig. 3A), indicating that the additional binding interface provided by the SH3 domain in Neffins has an inhibitory impact on this Nef function that is involved in the impairment of the immunological synapse. Interestingly, whereas Nef-GFP was localized mainly at the cell cortex and in the perinuclear region both in control cells (Fig. 3A, no sdAb) and in cells expressing sdAb19, the coexpression of Neffin B6 or C1 resulted in a more diffuse cytoplasmic distribution of Nef-GFP (Fig. 3A, left), suggesting that Neffins affect cellular functions of Nef in T cells through the alteration of its intracellular distribution.

Neffins and sdAb19 inhibit the Nef-mediated enhancement of virus infectivity. Since the positive impact of Nef on virus infectivity depends on the integrity of both the Leu-based and poly-Pro motifs of the protein (24, 35), we also addressed if Neffins were able to affect the Nef-mediated infectivity enhancement of new progeny virions. The ability of Neffins and sdAb19 to affect virus infectivity when expressed in virus-producing cells was investigated in a single-round infection assay. Nef-deleted reporter viruses carrying the gene encoding GFP were produced in the absence or presence of Nef expressed in *trans* and in combination with a fixed concentration of Neffins or sdAb19 (1:3 ratio of the plasmids encoding Nef and Neffins or sdAb19, respectively). As expected, viruses provided with the HIV-1 envelope produced from Nef-expressing cells showed a net increase of virus infectivity, whereas Nef expression did not increase the infectivity of viruses pseudotyped with the VSV-G envelope (Fig. 4). When HIV-1 *env*-containing viruses were produced in the presence of

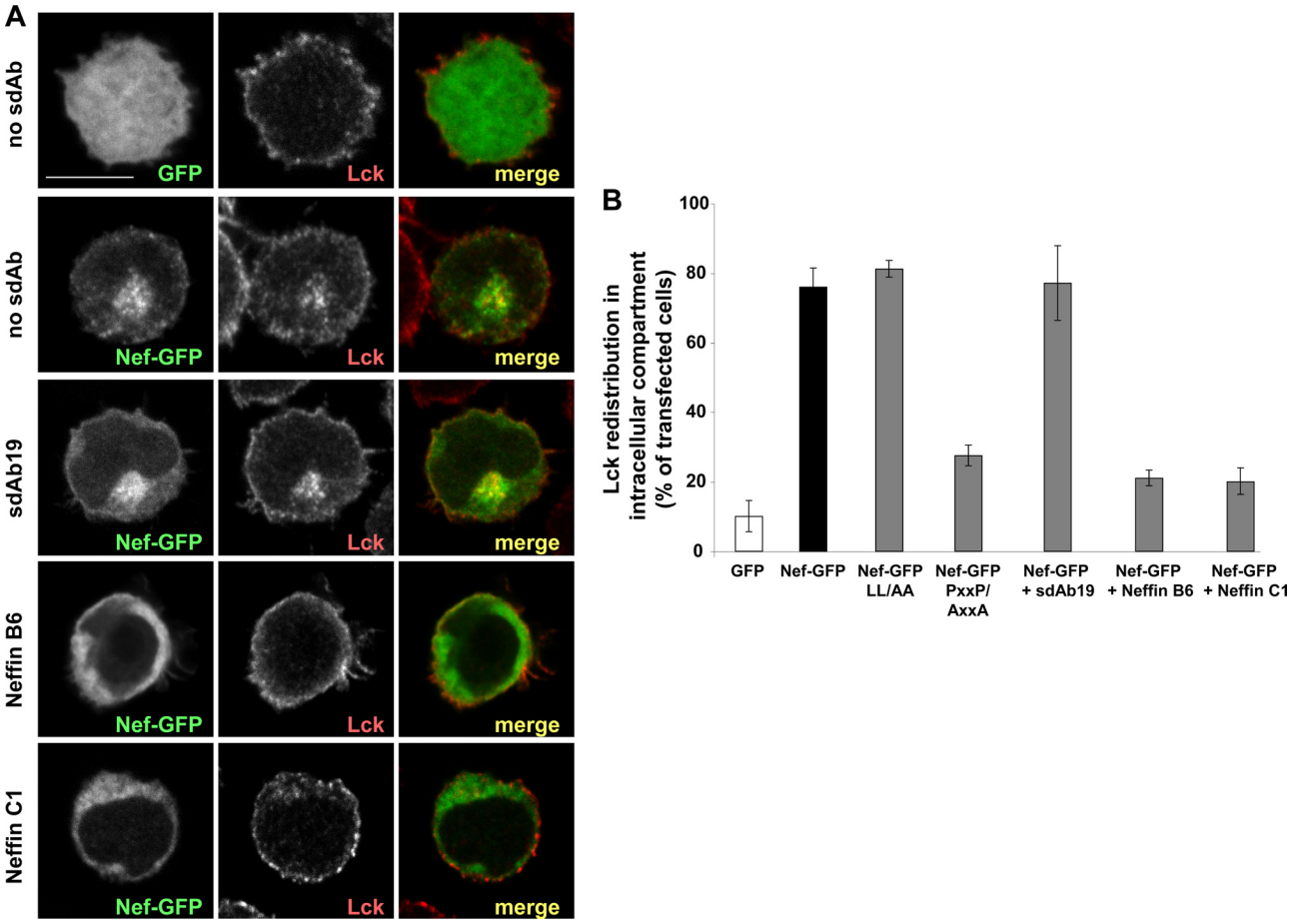

FIG 3 Neffins inhibit Nef-mediated mislocalization of Lck. Jurkat T cells were transfected with plasmids for the expression of either wild-type or mutated Nef-GFP in combination with plasmids for the expression of sdAb19, Neffin B6, or Neffin C1 (1:1). (A) Subcellular distribution of Nef-GFP (in green) and Lck (in red) in GFP- or Nef-GFP-transfected Jurkat cells. Representative images of cells expressing GFP (used as a control) or Nef-GFP alone (no sdAb) or in combination with sdAb19, Neffin B6, or Neffin C1 (as indicated) are shown. (B) Percentages of transfected cells showing Lck mislocalization were calculated by the observation of 50 GFP-positive cells for each condition. Results are expressed as the percentage of total GFP-positive cells. Values are the means from 3 independent experiments. Error bars represent 1 SD from the means.

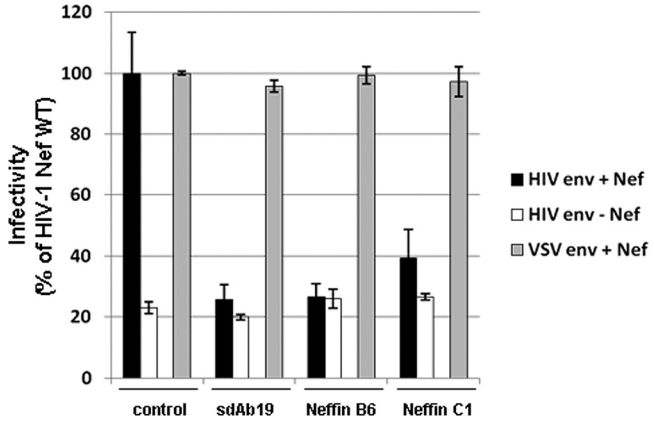

FIG 4 Neffins and sdAb19 inhibit Nef-mediated enhancement of virus infectivity. Single-round GFP reporter viruses, pseudotyped with either HIV-1 Env or VSV-G, were produced in 293T cells in the absence or presence of the plasmids expressing sdAb19 or Neffins. Forty-eight hours later, viruses were pelleted from cell culture supernatants and were used to infect HeLa-CD4 cells. The percentages of GFP-positive infected cells then were measured by flow cytometry 60 h later. Viral infectivity was normalized to that of viruses produced in the presence of Nef. Values are the means from 3 independent experiments. Error bars represent 1 SD from the means.

Neffin C1 or B6, an 80 and 95% decrease, respectively, of the specific effect of Nef on virus infectivity was observed. A similarly strong decrease of virus infectivity was observed when viruses were produced in cells transfected with the same ratio of the plasmid encoding the parental sdAb19. These results show that Neffins can abrogate the Nef-induced enhancement of HIV-1 infectivity; however, similarly to CD4 modulation, they do not show greater potency than sdAb19 in this function of Nef.

Neffins and sdAb19 inhibit macrophage fusion and podosome rosette formation induced by Nef in macrophages. Since the poly-Pro-dependent binding of Nef to Hck, the Src tyrosine kinase that is specifically expressed in macrophages, is the best-characterized interaction of Nef with cellular proteins containing SH3 domains (23), we decided to investigate the potential inhibitory effects of Neffins on the perturbations induced by Nef on specific functions of macrophages. For this, we expressed Nef in the RAW264.7 macrophage cells in which the expression of Nef was sufficient to recapitulate all of the Nef-dependent alterations observed in HIV-1-infected primary human monocyte-derived macrophages (40). As previously reported (40), Nef expression triggered the formation of multinucleated macrophages with an

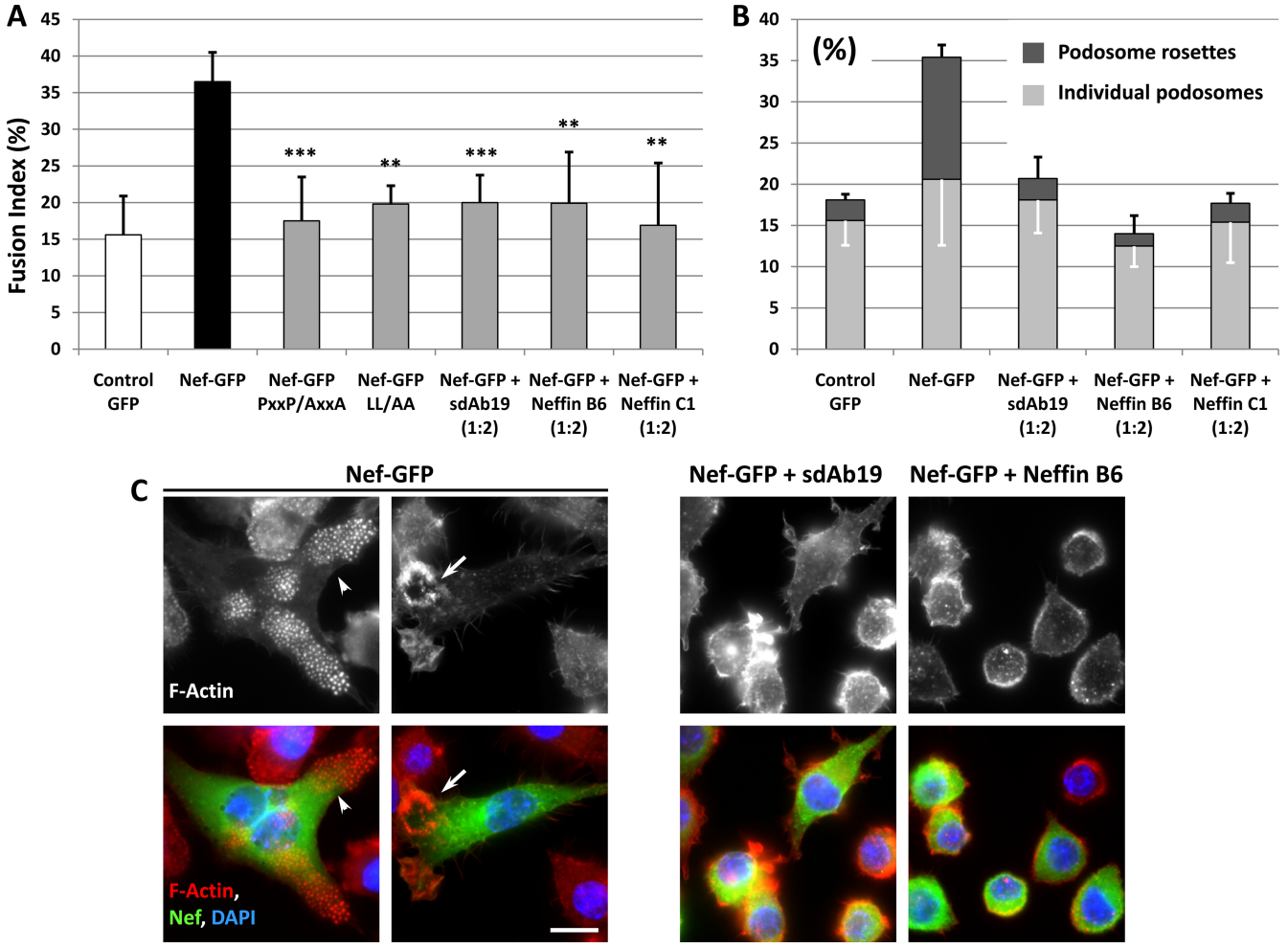

FIG 5 sdAb19 and Neffins inhibit Nef-induced cell fusion and podosome rosette formation in macrophages. (A to C) RAW264.7 macrophages were transiently transfected with a pEGFP vector (control GFP) in combination with plasmids for the expression of wild-type or mutated HA-tagged Nef and for the expression of sdAb19, Neffin B6, or Neffin C1 (1:2 ratio). Cells then were immunostained with anti-HA antibodies and with Alexa Texas red-coupled phalloidin for F-actin and DAPI for nuclei. (A) Quantification of cell fusion index evaluated 48 h after transfection ($n = 5$). (B) Percentage of cells with individual podosomes or podosome rosettes 24 h after transfection ($n = 3$). (C) Immunofluorescence microscopy of RAW264.7 macrophages. F-actin is shown in red, Nef-HA in green, and nuclei in blue (DAPI). White arrowheads show a cluster of individual podosomes, and arrows show a podosome rosette. Bar, 10 μm.

increase of more than 2-fold in the fusion index compared to control cells, and this effect was dependent on the poly-Pro motif that was required for interaction with Hck (Fig. 5A and C). Interestingly, the NefLL/AA variant, with substitutions of the two leucine residues of the Leu-based motif required for Nef interaction with the clathrin-associated AP complexes, was also deficient for macrophage fusion (Fig. 5A). This result demonstrates that the Nef-induced fusion of macrophages is related, in addition to the Nef effects on the Hck-dependent signaling pathway, to the perturbations provoked by Nef expression on intracellular trafficking. When RAW264.7 cells were transfected with the Nef-GFP expression plasmid in combination with plasmids for the expression of sdAb19 or Neffins, a significant decrease of the cell fusion index was measured (Fig. 5A). These results show that both Neffins, as well as the parental sdAb19, are able to inhibit the Nef-triggered fusion of macrophages.

We next examined whether the Neffins and sdAb19 also inhibited the actin remodelling phenotypes that are characteristic of the activation of endogenous Hck by Nef in RAW264.7 macrophages (43). We have previously shown that Nef-expressing macrophages rearranged their podosomes (Fig. 5C, arrowhead) into podosome rosettes (arrow) by the activation of the p61 isoform of Hck (6, 40). When cells expressed Nef-HA in combination with Neffin B6, Neffin C1, or sdAb19, a significant decrease of the number of cells with podosome rosettes was observed (Fig. 5B and C). Taken together, these results show that both Neffins and sdAb19 are able to inhibit the Nef phenotypes induced, at least in part, by Hck activation in macrophages. They also reveal that the Nef-induced phenotype of macrophage fusion was dependent of both Leu-based and poly-Pro motifs, indicating that this effect is related to the functional perturbations induced by Nef on both intracellular trafficking and signaling pathways.

Neffins and sdAb19 restore the phagocytosis function of macrophages expressing Nef. Finally, the anti-Nef inhibitory activity of Neffins and sdAb19 was explored on the reduction of phagocytosis induced by Nef expression in macrophages (28). The efficiency of the cell association and phagocytosis of particles was evaluated in RAW264.7 cells expressing Nef by fluorescence mi-

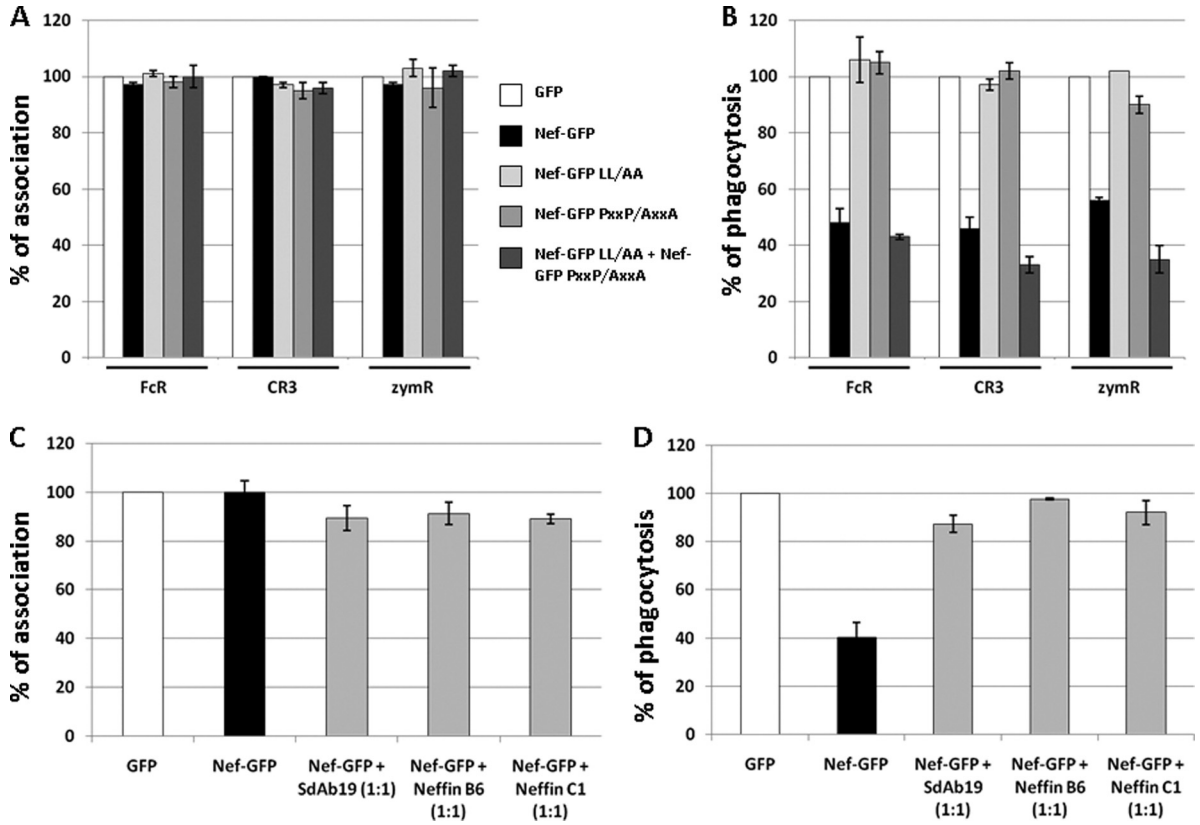

FIG 6 sdAb19 and Neffins restore efficient phagocytosis in macrophages expressing Nef. (A and B) Motifs of Nef involved in phagocytosis inhibition. RAW264.7 macrophages transiently expressing GFP or wild-type or mutated Nef-GFP were processed for the phagocytosis of IgG-RBCs, C3bi-RBCs, or zymosan for 60 min at 37°C. (C and D) RAW264.7 macrophages transiently expressing GFP or Nef-GFP in combination with sdAb19, Neffin B6, or Neffin C1 were processed for the phagocytosis of IgG-RBCs. The efficiencies of association (A and C) and phagocytosis (B and D) were calculated for 50 GFP-positive and 50 GFP-negative cells (GFP control). Results are expressed as a percentage of control GFP-negative cells. Values are the means from 3 independent experiments. Error bars represent 1 SD from the means.

croscopy after interactions with IgG- or complement-opsonized sheep red blood cells or with fluorescent zymosan (heat-inactivated yeast). As reported in Fig. 6B, a significant reduction of FcR- and CR3-mediated phagocytosis, as well as uptake of zymosan, was observed in Nef-expressing cells, whereas Nef had no effect on the initial binding of the particles to cells (Fig. 6A). In agreement with previous results showing that this Nef activity was related to a decrease of the recruitment of AP-1-positive endosomes at the phagocyte cup (28), the NefLL/AA mutant was deficient for the inhibition of phagocytosis (Fig. 6B). Interestingly, the NefPxxP/AxxA mutant, with substitutions of the proline residues of the poly-Pro motif, also failed to reduce macrophage phagocytosis (Fig. 6B). These results indicate that the Nef-induced inhibition of phagocytosis is related, in addition to the Nef effects on the endocytic pathway, to the perturbations provoked by Nef expression on signaling pathways in macrophages. Interestingly, an efficient reduction of phagocytosis, equivalent to that measured in cells expressing the wild-type Nef protein, was measured by the coexpression of both NefLL/AA and NefPxxP/AxxA mutants (Fig. 6B), confirming that Nef acts on different intracellular pathways for alterations of phagocytosis in macrophages.

To analyze the inhibitory activity of Neffins and sdAb19 on the Nef-induced reduction of phagocytosis, RAW264.7 cells were cotransfected with Nef-GFP and sdAb19 or Neffin expression plasmids in a 1:1 ratio and then submitted to the phagocytosis of IgG-opsonized sheep red blood cells. As shown in Fig. 6D, the rate of phagocytosis in cells coexpressing Neffin B6, Neffin C1, or sdAb19 was almost totally restored to a level equivalent to that of the control cells. We checked that the association of particles on macrophages was not affected by the expression of Neffins or sdAb19 (Fig. 6C). These results indicate that sdAb19 and Neffins are both able to counteract the negative effect of Nef on phagocytosis by macrophages.

Neffins and sdAb19 disrupt interactions of Nef with AP-1 complex and Hck. Taken together, the results reported in Fig. 5 and 6 demonstrated that the Nef-induced alterations provoked by Nef on macrophage functions were dependent on both the Leu-based and poly-Pro motifs, suggesting that the inhibitory activity of Neffins and sdAb19 on these functions is related to the modulation of the specific interactions of Nef with both AP complexes and Hck. Therefore, the impact of Neffins and sdAb19 on these interactions was challenged using an *in vitro* pulldown assay. Recombinant Nef fused to GST was expressed in *E. coli* (Fig. 7A, lower), immobilized on GSH-Sepharose beads, and then tested for interactions with native AP-1 complexes and Hck from a lysate of human monocytic THP-1 cells (Fig. 7A, right) in the presence of increasing amounts of recombinant sdAb19 or Neffins. Bound proteins were analyzed by Western blotting with anti-γ-adaptin

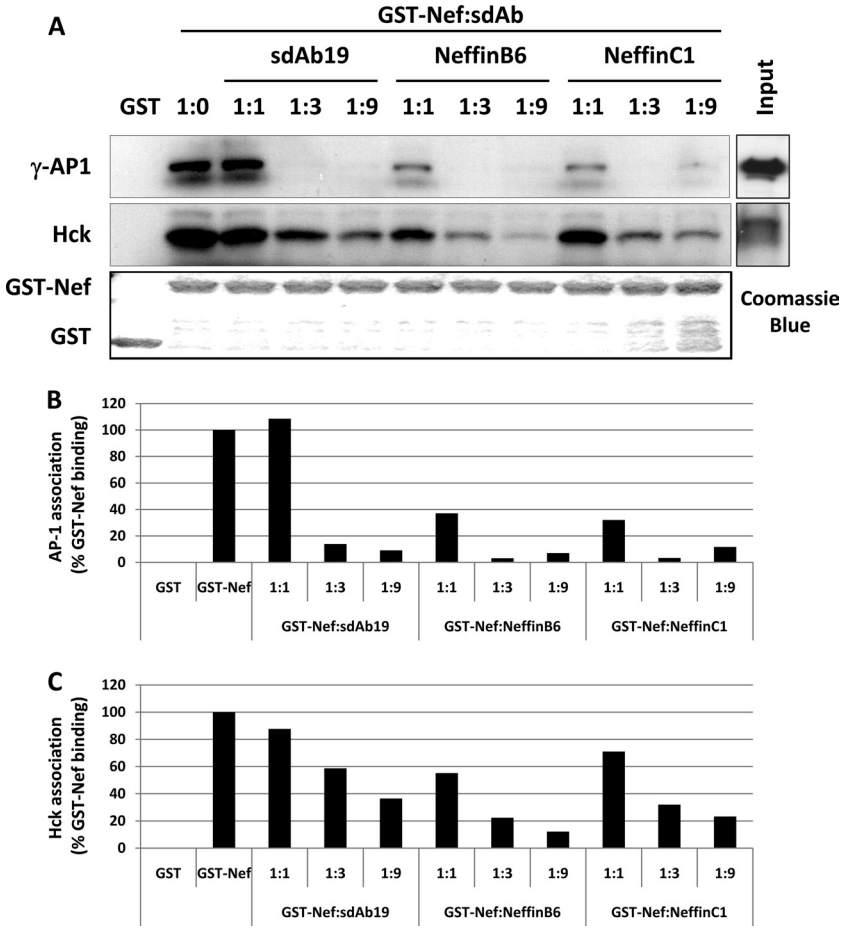

FIG 7 Neffins and sdAb19 inhibit Nef association with AP-1 and Hck. (A) Purified recombinant GST or GST-Nef was immobilized on glutathione Sepharose beads (lower panel; Coomassie blue) and then were incubated with THP-1 cell lysates in the presence of increasing amounts of sdAb19 or Neffins. Bound material (left panels) and total lysates (right panels) were subjected to Western blotting with anti-AP-1 (upper panels) or anti-Hck (middle panels) antibody. The percentages of association of AP-1 (B) or Hck (C) with GST-Nef were normalized to the association without inhibitor (100%).

and anti-Hck antibodies (Fig. 7A, upper and middle, respectively).

As reported previously (28), both the full-length and a cleaved form of γ-adaptin, which plays a role in the regulation of recycling from endosomes to the plasma membrane, were pulled down by GST-Nef but not by the GST control (Fig. 7A, upper). At an equimolar ratio with GST-Nef (1:1) (Fig. 7B), sdAb19 was not able to inhibit Nef-AP-1 interaction, whereas a significant inhibition (65%) of the Nef recruitment of γ-adaptin was measured with both Neffins. By increasing the amount of Neffins or sdAb19 to 1:3 or 1:9, we could totally block the Nef-AP-1 interaction. Even if the interaction between Nef and AP-1 does not depend on the poly-Pro motif but rather required the Leu-based motif, these results indicate that the presence of the SH3 part in Neffins helps the inhibition of the interaction of Nef with AP-1 complexes.

Like AP-1 complexes, Hck was specifically pulled down by GST-Nef from a THP-1 cell lysate (Fig. 7A, middle). An efficient dose-dependent inhibition of this interaction was evidenced with both Neffins and also with sdAb19 (Fig. 7C). The latter result indicates that the poly-Pro motif is not fully accessible for interaction with the SH3 domain of Hck after the binding of sdAb19 to Nef. However, a comparison of Hck binding to Nef in the presence of Neffins or sdAb19 revealed that Neffins were more effective for the inhibition of this interaction (Fig. 7A and C).

Taken together, the results reported in Fig. 7 show that both Neffins and sdAb19 are able to impair, at least *in vitro*, the specific interactions of Nef with AP-1 complex and Hck. They also suggest that the fusion of the modified SH3 domains to sdAb19 results in a higher affinity and/or avidity of sdAb19 for Nef.

DISCUSSION

In the present study, we report the characterization of the inhibitory activity of the anti-Nef single-domain antibody fragment sdAb19 and its derivatives fused to modified SH3 domains, so-called Neffins, on distinct intracellular functions of HIV-1 Nef, including Nef-induced alterations of T lymphocyte and macrophage functions. These anti-Nef inhibitors were able to block several functions of Nef that mediate the effects of this viral protein in HIV-1 pathogenesis. Indeed, Neffins showed potent effects on the Nef-induced downregulation of the cell surface expression of both CD4 and MHC-I molecules, and they also inhibited the Nef-induced mislocalization of the T cell-specific Lck kinase. Neffins were also able to drastically reduce the Nef-mediated enhancement of HIV-1 infectivity. Finally, Neffins showed important in-

hibitory effects in macrophages. First, they inhibited macrophage fusion and the formation of podosome rosettes induced by Nef. Second, they restored the phagocytosis activity inhibited by Nef in macrophages. Neffins likely inhibited these Nef effects on macrophage functions through their ability to inhibit interactions of Nef with both AP-1 complex and Hck.

Some of the Nef functions examined in this study, such as MHC-I downregulation, the mislocalization of Lck, and association with Hck or AP-1, were more efficiently inhibited by Neffins than by the parental sdAb19. On the other hand, other Nef functions, such as CD4 downregulation, were equally well suppressed by Neffins and sdAb19. These differences most likely reflect the capacity of Neffins to occupy a larger area on the surface of Nef and thereby mask additional functional determinants, especially the Nef poly-Pro motif. They could also reflect an increased overall strength of binding to Nef provided by the extended interaction interface, as evidenced by the ability of Neffins to counteract some Nef proteins that were not affected by sdAb19. Indeed, biochemical studies on the Neffin-Nef interaction have revealed a more than 25-fold increase in binding affinity compared to that of the sdAb19-Nef complex, which is mainly due to the significantly slower dissociation of the Neffin-Nef complex (Järviluoma et al., unpublished). Furthermore, it has been suggested that Nef functions involve transitions between alternative conformations (17), thus a higher capacity to restrain the flexibility of the Nef protein might contribute to the increased potency of Neffins in inhibiting some effects of Nef. Similarly, efficient Nef inhibitors engineered for the targeting of the multiple interaction sites of Nef were recently reported (4).

The downregulation of MHC-I molecules is a common function developed by several viruses, including herpesviruses and poxviruses (44), for escape from the immune system. For HIV-1, this important function is mediated by Nef, and the development of an antiviral strategy targeting Nef needs to inhibit this function of Nef to help the immune system to target infected cells. The parental sdAb19 was not able to restore physiological MHC-I surface expression in the presence of Nef, probably because it was unable to mask the two main motifs (i.e., $E_{62}EEE_{65}$ and $P_{72}xxP_{75}$) required for this Nef function (26, 29, 32). In contrast, the fusion of sdAb19 to RRT-SH3 domains in Neffins led to the specific targeting of the poly-Pro motif of Nef, which is involved in the recruitment of the Src family kinase that is required for the induction of MHC-I endocytosis by Nef (8). Nef association with AP-1 complexes was also involved in the mechanism of Nef-induced MHC-I downregulation (29, 33, 42). The N-terminal acidic cluster ($E_{62}EEE_{65}$) of Nef and a single residue in the polyproline helix, P_{78}, which is not required for the SH3-binding activity of Nef, also participate in the downregulation of MHC-I through direct or indirect interactions with AP-1 (29, 41). The close proximity of both $E_{62}EEE_{65}$ and P_{78} with the $P_{72}xxP_{75}$ SH3-binding motif could explain why Neffins inhibited AP-1 binding to Nef with a higher efficiency than that of sdAb19. Indeed, this effect of Neffins may be due to their ability to alter the folding of Nef, thus preventing the ability of $E_{62}EEE_{65}$ and P_{78} motifs to recognize AP-1 and leading to the inhibition of Nef-induced MHC-I downregulation (29). The fact that Neffins are still active for the inhibition of cell surface CD4 downregulation as efficiently as sdAb19 indicates that there is no competitive effect between the respective RRT-SH3 and sdAb19 parts of Neffins on Nef. Therefore, Neffins are probably able to simultaneously target the acidic cluster, the polyproline-rich region comprised of residues between P_{72} and P_{78}, and the conformational epitope recognized by sdAb19 on Nef. This targeting may also affect cellular functions of Nef in T cells through the alteration of its intracellular distribution.

Similarly, the parental sdAb19 was not able to counteract the mislocalization of the TCR-proximal Lck kinase in endosomal compartments induced by Nef in T cells, probably because it was unable to mask the poly-Pro motif required for this Nef function (23, 27, 30). In contrast, the addition of the RRT-SH3 domains in Neffins led to the specific targeting of this motif of Nef and thus the inhibition of the Lck mislocalization, a function responsible, at least in part, for the alterations of the organization and function of the immunological synapse formed between infected T cells and antigen-presenting cells (34, 37). Moreover, our preliminary results indicate that the decrease observed in the formation of conjugates between T cells expressing Nef and B cells used as antigen-presenting cells was also inhibited by the coexpression of Neffins (data not shown).

In a recent study, we showed that Nef expression induced the fusion of infected macrophages, leading to the formation of multinucleated giant cells through the activation of the p61 isoform of Hck (40). The function of these giant cells in HIV-1 pathogenesis is not well established, but they have been identified in several tissues from AIDS patients, such as the brain, and they have been proposed as markers of the progression of HIV-1-induced dementia (30, 31). The formation of such giant cells by an Hck-dependent mechanism also could contribute to the establishment of latent virus reservoirs in some tissues (40). In addition, the Nef-induced activation of p61Hck at the level of lysosomes led to the formation of podosome rosettes (40). These structures are involved in the proteolytic degradation of the extracellular matrix and are required for macrophage migration in dense and compact three-dimensional environments (7, 38, 39). As expected, both the fusion of macrophages and the formation of podosome rosettes are dependent on the poly-Pro motif of Nef that is required for Hck binding (40). More surprisingly, we show here that the NefLL/AA mutant also was impaired for the cell fusion phenotype, indicating that this function of Nef involves the recruitment and activation of p61Hck at the lysosomes as well as some other effectors of Nef that are dependent on the Leu-based motif that is required for interactions with endosomal AP complexes. We speculate that Nef is able to disturb the intracellular trafficking and the cell surface expression of molecules regulating membrane fusion in macrophages. Therefore, the total inhibition of the effect of Nef on giant cell formation and podosome rosette induction observed by coexpressing Neffins or sdAb19 in macrophages is not surprising, since we show here that they are able to disrupt interactions of Nef with both AP complexes and Hck.

Similarly, we revealed here that the NefLL/AA and NefPxxP/AxxA mutants failed to inhibit macrophage phagocytosis. While we previously showed that this Nef-induced inhibition was dependent on the Leu-based motif (28), these data indicate that it is also dependent on the poly-Pro motif. The phagocytosis process and the fusion of macrophages are complex processes that show some similarities (reviewed in reference 14). The two processes involve the reorganization of the actin cytoskeleton and require Hck activation. During Fcγ receptor-mediated phagocytosis, p59Hck is initially recruited at the phagocytic cup, while p61Hck is recruited in phagosomes (11). The specific role of Hck in phagocytosis is still unclear, but the sequential recruitment of p59 and

p61Hck likely plays a major role in this process. By interacting with the two isoforms of Hck through its poly-Pro motif (40), Nef could have a detrimental effect on phagocytosis. Interestingly, by coexpressing the two NefLL/AA and PxxP/AxxA mutants, we could rescue the inhibitory effect of Nef on phagocytosis. Two hypotheses could be suggested to explain this result. First, Nef could inhibit at least two steps of the phagocytosis process, and these two steps may involve the Leu-based and poly-Pro motifs of Nef. Second, Nef oligomerization could be required for the inhibition of phagocytosis, and the formation of oligomers between the two Nef mutants would lead to the reconstitution of fully active Nef proteins. Again, the impairment of phagocytosis induced by Nef was efficiently inhibited by sdA19 and Neffins and likely results from the inhibition of the interactions of Nef with AP-1 complexes and Hck.

While we previously showed that sdAb19 was able to interfere with the association of HIV-1 Nef with the cellular p21-activated kinase 2 (PAK2) that is involved in the resulting inhibitory effect of Nef on actin remodeling in T lymphocytes (2), we report here that Neffins, as well as the parental sdAb19, are able to disrupt interactions of Nef with clathrin-associated AP complexes and the phagocyte-specific Hck tyrosine kinase from CD4-positive myeloid cells. The latter result indicates that the poly-Pro motif is not fully accessible for interaction with the SH3 domain of Hck after the binding of sdAb19 to Nef. However, the quantitative comparison of Hck binding to Nef in the presence of Neffins or sdAb19 revealed that Neffins were more effective for the inhibition of this interaction. This observation suggests that the fusion of the modified SH3 domains to sdAb19 in Neffins results in a higher affinity and/or avidity of sdAb19 for Nef. Taken together, these results demonstrate that Neffins are highly active for the inhibition of associations of HIV-1 Nef with its best-characterized cellular partners, which are responsible for most of the critical roles of Nef during the virus life cycle and in the progression of natural infection (reviewed in references 1 and 9).

In conclusion, Neffins, which are generated to improve the inhibitory activity of sdAb19, were able to inhibit all of the functions of Nef, including the cell surface downregulation of MHC-I, in both lymphoid and myeloid CD4-positive cells. When expressed in macrophages, Neffins inhibited the Nef-induced formation of multinucleated giant cells and podosome rosettes, and they also rescued the inhibitory activity of Nef on phagocytosis through the disruption of specific interactions of Nef with both AP complexes and Hck. Taken together, these results demonstrate that it is possible to inhibit all Nef functions, both in T lymphocytes and macrophages, with a single ligand, and this represents an efficient tool to develop new antiviral strategies targeting Nef.

ACKNOWLEDGMENTS

We thank Hamasseh Shirvani and Stefano Marullo (Cochin Institute, Paris, France) for the generous gift of reagents.

This work was supported by INSERM, CNRS, Université Paris-Descartes, and grants from the Agence Nationale de Recherche sur le SIDA (ANRS) (S.B., D.B., F.N., and I.M.P.). J.B. was supported by a Bourse de Docteur Ingénieur (BDI) that was cofunded by CNRS and INSERM. C.V. and S.R. were supported by a fellowship from Sidaction, while C.G. and J.M. were supported by a fellowship from ANRS.

REFERENCES

1. **Arhel NJ, Kirchhoff F.** 2009. Implications of Nef: host cell interactions in viral persistence and progression to AIDS. Curr. Top. Microbiol. Immunol. **339**:147–175.
2. **Bolte S, Cordelières FP.** 2006. A guided tour into subcellular colocalization analysis in light microscopy. J. Microsc. **224**:213–232.
3. **Bouchet J, et al.** 2011. Inhibition of the Nef regulatory protein of HIV-1 by a single-domain antibody. Blood **117**:3559–3568.
4. **Breuer S, et al.** 2011. Molecular design, functional characterization and structural basis of a protein inhibitor against the HIV-1 pathogenicity factor Nef. PLoS One **6**:e20033.
5. **Burtey A, et al.** 2007. Dynamic interaction of HIV-1 Nef with the clathrin-mediated endocytic pathway at the plasma membrane. Traffic **8**:61–76.
6. **Cougoule C, et al.** 2005. Activation of the lysosome-associated p61Hck isoform triggers the biogenesis of podosomes. Traffic **6**:682–694.
7. **Cougoule C, et al.** 2010. Three-dimensional migration of macrophages requires Hck for podosome organization and extracellular matrix proteolysis. Blood **115**:1444–1452.
8. **Dikeakos JD, et al.** 2010. Small molecule inhibition of HIV-1-induced MHC-I down-regulation identifies a temporally regulated switch in Nef action. Mol. Biol. Cell **21**:3279–3292.
9. **Foster JL, Denial SJ, Temple BRS, Garcia JV.** 2011. Mechanisms of HIV-1 Nef function and intracellular signaling. J. Neuroimmune Pharmacol. **6**:230–246.
10. **Gavegnano C, Schinazi RF.** 2009. Antiretroviral therapy in macrophages: implication for HIV eradication. Antivir. Chem. Chemother. **20**:63–78.
11. **Guiet R, et al.** 2008. Hematopoietic cell kinase (Hck) isoforms and phagocyte duties-from signaling and actin reorganization to migration and phagocytosis. Eur. J. Cell Biol. **87**:527–542.
12. **Haller C, Rauch S, Fackler OT.** 2007. HIV-1 Nef employs two distinct mechanisms to modulate Lck subcellular localization and TCR induced actin remodeling. PLoS One **2**:e1212.
13. **Hanna Z, et al.** 1998. Nef harbors a major determinant of pathogenicity for an AIDS-like disease induced by HIV-1 in transgenic mice. Cell **95**:163–175.
14. **Helming L, Gordon S.** 2009. Molecular mediators of macrophage fusion. Trends Cell Biol. **19**:514–522.
15. **Hiipakka M, Huotari P, Manninen A, Renkema GH, Saksela K.** 2001. Inhibition of cellular functions of HIV-1 Nef by artificial SH3 domains. Virology **286**:152–159.
16. **Hiipakka M, Poikonen K, Saksela K.** 1999. SH3 domains with high affinity and engineered ligand specificities targeted to HIV-1 Nef. J. Mol. Biol. **293**:1097–1106.
17. **Horenkamp FA, et al.** 2011. Conformation of the dileucine-based sorting motif in HIV-1 Nef revealed by intermolecular domain assembly. Traffic **12**:867–877.
18. **Horita DA, et al.** 1998. Solution structure of the human Hck SH3 domain and identification of its ligand binding site. J. Mol. Biol. **278**:253–265.
19. **Janvier K, et al.** 2003. HIV-1 Nef stabilizes the association of adaptor protein complexes with membranes. J. Biol. Chem. **278**:8725–8732.
20. **Laguette N, et al.** 2009. Nef-induced CD4 endocytosis in human immunodeficiency virus type 1 host cells: role of p56lck kinase. J. Virol. **83**:7117–7128.
21. **Laguette N, Benichou S, Basmaciogullari S.** 2009. Human immunodeficiency virus type 1 Nef incorporation into virions does not increase infectivity. J. Virol. **83**:1093–1104.
22. **Laguette N, Brégnard C, Benichou S, Basmaciogullari S.** 2010. Human immunodeficiency virus (HIV) type-1, HIV-2 and simian immunodeficiency virus Nef proteins. Mol. Aspects Med. **31**:418–433.
23. **Lee CH, et al.** 1995. A single amino acid in the SH3 domain of Hck determines its high affinity and specificity in binding to HIV-1 Nef protein. EMBO J. **14**:5006–5015.
24. **Madrid R, et al.** 2005. Nef-induced alteration of the early/recycling endosomal compartment correlates with enhancement of HIV-1 infectivity. J. Biol. Chem. **280**:5032–5044.
25. **Manders EM, Stap J, Brakenhoff GJ, van Driel R, Aten JA.** 1992. Dynamics of three-dimensional replication patterns during the S-phase, analysed by double labelling of DNA and confocal microscopy. J. Cell Sci. **103**:857–862.
26. **Mangasarian A, Piguet V, Wang JK, Chen YL, Trono D.** 1999. Nef-induced CD4 and major histocompatibility complex class I (MHC-I)

down-regulation are governed by distinct determinants: N-terminal alpha helix and proline repeat of Nef selectively regulate MHC-I trafficking. J. Virol. **73**:1964–1973.
27. **Mayer BJ.** 2001. SH3 domains: complexity in moderation. J. Cell Sci. **114**:1253–1263.
28. **Mazzolini J, et al.** 2010. Inhibition of phagocytosis in HIV-1-infected macrophages relies on Nef-dependent alteration of focal delivery of recycling compartments. Blood **115**:4226–4236.
29. **Noviello CM, Benichou S, Guatelli JC.** 2008. Cooperative binding of the class I major histocompatibility complex cytoplasmic domain and human immunodeficiency virus type 1 Nef to the endosomal AP-1 complex via its mu subunit. J. Virol. **82**:1249–1258.
30. **Orenstein JM.** 2001. The macrophage in HIV infection. Immunobiology **204**:598–602.
31. **Orenstein JM, Wahl SM.** 1999. The macrophage origin of the HIV-expressing multinucleated giant cells in hyperplastic tonsils and adenoids. Ultrastruct. Pathol. **23**:79–91.
32. **Piguet V, et al.** 2000. HIV-1 Nef protein binds to the cellular protein PACS-1 to downregulate class I major histocompatibility complexes. Nat. Cell Biol. **2**:163–167.
33. **Roeth JF, Williams M, Kasper MR, Filzen TM, Collins KL.** 2004. HIV-1 Nef disrupts MHC-I trafficking by recruiting AP-1 to the MHC-I cytoplasmic tail. J. Cell Biol. **167**:903–913.
34. **Rudolph JM, Eickel N, Haller C, Schindler M, Fackler OT.** 2009. Inhibition of T-cell receptor-induced actin remodeling and relocalization of Lck are evolutionarily conserved activities of lentiviral Nef proteins. J. Virol. **83**:11528–11539.
35. **Saksela K, Cheng G, Baltimore D.** 1995. Proline-rich (PxxP) motifs in HIV-1 Nef bind to SH3 domains of a subset of Src kinases and are required for the enhanced growth of Nef+ viruses but not for down-regulation of CD4. EMBO J. **14**:484–491.
36. **Schwartz O, Marechal V, Le Gall S, Lemonnier F, Heard JM.** 1996. Endocytosis of major histocompatibility complex class I molecules is induced by the HIV-1 Nef protein. Nat. Med. **2**:338–342.
37. **Thoulouze MI, et al.** 2006. Human immunodeficiency virus type-1 infection impairs the formation of the immunological synapse. Immunity **24**:547–561.
38. **Van Goethem E, et al.** 2011. Macrophage podosomes go 3D. Eur. J. Cell Biol. **90**:224–236.
39. **Van Goethem E, Poincloux R, Gauffre F, Maridonneau-Parini I, Le Cabec V.** 2010. Matrix architecture dictates three-dimensional migration modes of human macrophages: differential involvement of proteases and podosome-like structures. J. Immunol. **184**:1049–1061.
40. **Vérollet C, et al.** 2010. HIV-1 Nef triggers macrophage fusion in a p61Hck- and protease-dependent manner. J. Immunol. **184**:7030–7039.
41. **Williams M, Roeth JF, Kasper MR, Filzen TM, Collins KL.** 2005. Human immunodeficiency virus type 1 Nef domains required for disruption of major histocompatibility complex class I trafficking are also necessary for coprecipitation of Nef with HLA-A2. J. Virol. **79**:632–636.
42. **Wonderlich ER, Williams M, Collins KL.** 2008. The tyrosine binding pocket in the adaptor protein 1 (AP-1) mu1 subunit is necessary for Nef to recruit AP-1 to the major histocompatibility complex class I cytoplasmic tail. J. Biol. Chem. **283**:3011–3022.
43. **Xu W, et al.** 2009. HIV-1 evades virus-specific IgG2 and IgA responses by targeting systemic and intestinal B cells via long-range intercellular conduits. Nat. Immunol. **10**:1008–1017.
44. **Yewdell JW, Hill AB.** 2002. Viral interference with antigen presentation. Nat. Immunol. **3**:1019–1025.